A Platinum Open Access Journal for Organic Chemistry

Paper

Free to Authors and Readers | DOAJ Seal | *Arkivoc* **2024** (1) 202412348

Oxime esters on 4-nitrobenzaldehyde and 9,10-anthraquinone-2-carboxaldehyde templates: DNA- and albumin-binding and photocleavage studies

Stefanos Soultas,[a] Konstantinos Meliopoulos,[b] George Psomas,[c] Katerina R. Katsani,*[b] and Konstantina C. Fylaktakidou*[a]

[a] *Laboratory of Organic Chemistry, Faculty of Chemistry, Aristotle University of Thessaloniki, GR-54124 Thessaloniki, Greece*

[b] *Laboratory of Biochemistry and Molecular Virology, Molecular Biology and Genetics Department, Democritus University of Thrace, Dragana, GR-68100 Alexandroupolis, Greece*

[c] *Laboratory of Inorganic Chemistry, Faculty of Chemistry, Aristotle University of Thessaloniki, GR-54124 Thessaloniki, Greece*

Email: kkatsani@mbg.duth.gr, kfylakta@chem.auth.gr

Received mm-dd-yyyy **Accepted** mm-dd-yyyy **Published on line** mm-dd-yyyy

Dates to be inserted by editorial office

Abstract

A series of novel oxime esters based on 4-nitrobenzaldehyde and 9,10-anthraquinone-2-carboxaldehyde templates have been synthesized. In addition to aroyl esters, isobutanoyl and 2-phenylpropanoyl moieties were introduced, yielding alkyloyl-esters capable of photocleaving DNA. Binding studies with DNA and serum albumin (BSA and HSA) revealed strong affinity for these biomolecules. Furthermore, protein photocleavage experiments demonstrated that both BSA and HSA undergo significant disruption upon UV-A irradiation (365 nm). These results highlight the potential of nitrobenzaldehyde- and anthaquinone-2-carboxaldehyde-derived oxime esters as promising candidates for photodynamic applications, including cancer therapy and microbial inactivation.

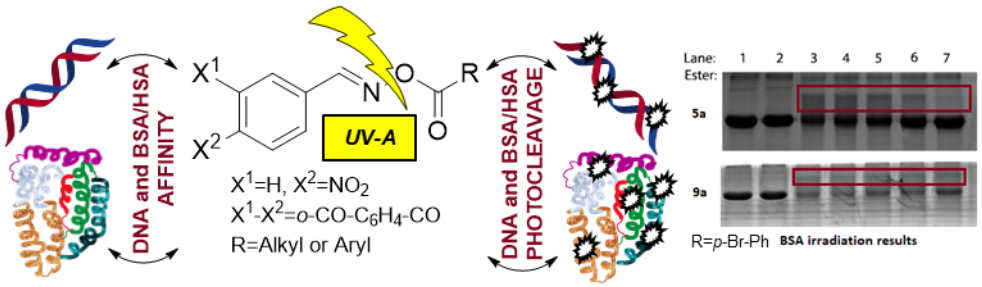

Keywords: Oxime esters, anthraquinone, 4-nitrobenzaldehyde, DNA-binding, DNA photocleavage, albumin binding/photocleavage

Introduction

Aldoxime or ketoxime carboxylic esters and ethers (R-R'C=N-O-R''), represented as **Ia-c** (Figure 1A), serve as valuable synthons in organic chemistry. These compounds undergo N-O bond homolysis (Figure 1B), generating iminyl radical intermediates (R-R'C=N˙), which participate in diverse chemical transformations. Their synthetic versatility has been demonstrated in the formation of 5- and 6-membered azaheterocycles and azahelicenes,[1–5] the production of γ-functionalized ketones[1,2,6] and their involvement in the synthesis of chiral amines and [2+2] cycloaddition reactions.[7]

Cyclic oxime lactones (**II**, isoxazolin-5(4*H*)-ones, Figure 1A) are known to yield alkynes,[8] whereas exocyclic oxime derivatives (**III**, Figure 1A) can undergo selective β-carbon scission relative to the iminyl radical, leading to the synthesis of aliphatic nitriles from specific substrates.[1,2,9,10] Depending on the structure of R and R', the iminyl radical may undergo rearrangement into a carbon-centered radical, enabling the formation of new C-C, C-O, C-N, C-S, C-X bonds.[11] Additionally, intermolecular syntheses of 3-, 4-, 5- and 6-membered heterocycles via metal-catalyzed processes involving oxime esters and ethers have been reported.[12,13]

Overall, oximes have been extensively utilized in the synthesis of amides, amines, nitriles, aromatic and non-aromatic heterocycles. In addition to their role in these transformations, they also facilitate the mild esterification of carboxylic acids and acylation of alcohols under neutral conditions,[14] further highlighting their significance as indispensable tools in organic synthesis.

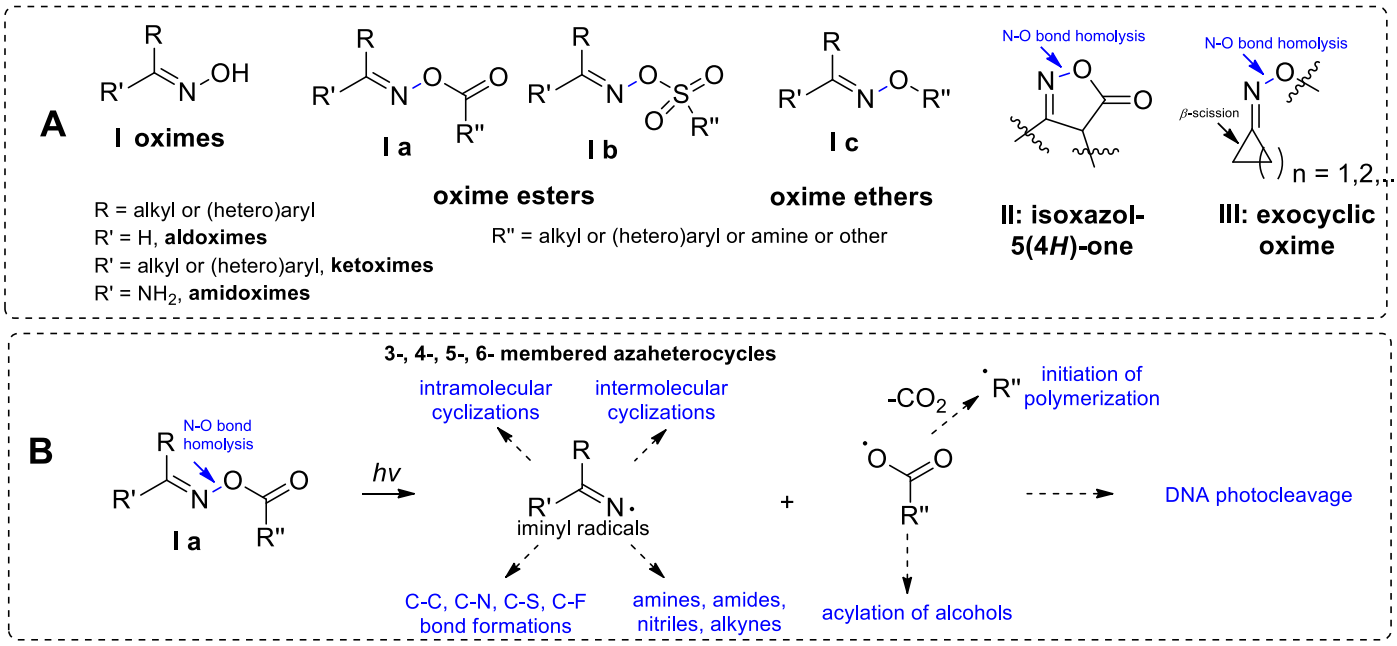

Figure 1. A: Structure and different categories of oximes (**I**) and their carboxylic and sulfonic esters (**Ia**, **Ib**), and ethers (**Ic**), oxime lactones (**II**) and exocyclic oximes (**III**); **B**: The way oxime esters are homolyzed to give radicals and their applications.

The fate of the oxygen-centered radical (˙O-C(=O)-R''), however, has been less frequently explored in chemical synthesis.[15] The decarboxylation efficiency of acyloxyl radicals allow the formation of aryl and alkyl radicals (R-R'C=N-O-C(=O)-R'' → ˙O-C(=O)-R'' → ˙R''), which participate in the initiation of polymer reactions. In this process, the substrate of the oxime moiety serves as the light photosensitizer (PS) that absorbs irradiation of a specific wavelength, most preferably visible light (Figure 1B).[16]

The fruitful photochemistry of oxime esters **1a** has similarly led to chemical and photobiological applications, particularly in DNA photodamage, a process known as DNA-photocleavage. As shown in Figure 1, bond homolysis of **1a** generates, in addition to the chemically useful iminyl radical (*vide supra*), an oxygen-centered radical. The work of Theodorakis et al., has demonstrated that this radical is most probably, though not exclusively, responsible for the DNA-attack. Aroyloxyl radicals are capable of reacting with DNA in a manner resembling hydroxyl radical-mediated damage, whereas alkyloxyl radicals were inactive towards DNA.[17] In the literature, the vast majority of oxime esters **Ia** (Figure 1B) featured aryl or heteroaryl R'' fragments and were efficient DNA-photocleavers, with their photoexcitation dependent on the light absorption of the oxime template (R-R'C=N-O).

Oxime template molecules containing simple *p*-NO_2-Ph moieties play important role at UV-A excitation (Figure 2A, **IVa**).[18] *o*-, *m*- and *p*-pyridine aldoximes, ethenone oxime, amidoxime,[19] and quinolines[20] (Figure 2A, **IVb,c**, respectively), as well as pyrenes,[21] tricyclic fussed aromatics and heteroaromatics,[22–24] and anthracene-9,10-diones (Figure 2A, **V**) bearing both Ar and HetAr conjugates,[24,25] were efficient DNA photocleavers at 312 and 365 nm.

Anthracene-9,10-dione represents a class of natural products and synthetic derivatives known for their activity as reactive oxygen species (ROS) regulators[26] and as chemotherapeutics.[27] These compounds also serve as organic PS that are easily excited to their triplet state, making them useful for photocatalysis,[28] and photodynamic therapy (PDT).[29,30] PDT is a cancer treatment that uses light as co-factor in combination with a photoactive compound and oxygen to induce cell damage.[31] Additionally, the application of this method has been extended to photoinactivation of bacteria.[32,33]

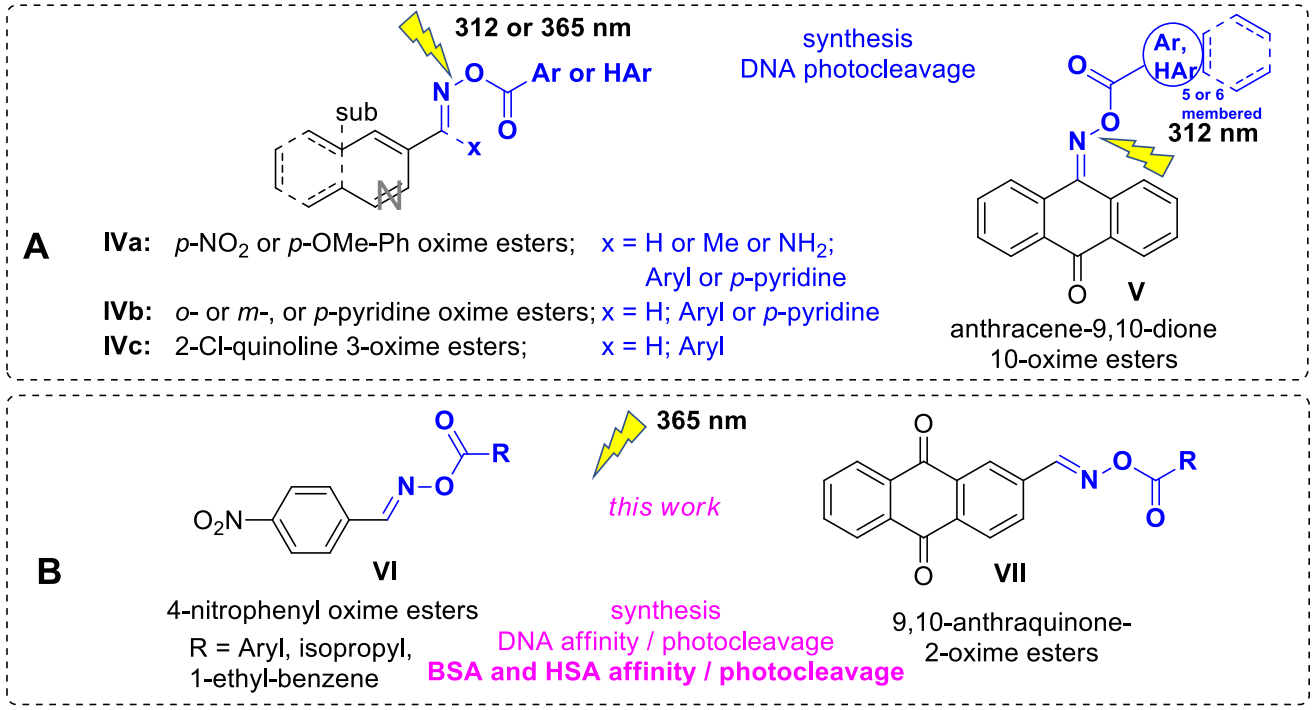

Figure 2. Oxime esters as DNA-photocleavers at various wavelengths; **A:** aryl, pyridine and quinoline oxime esters (**IVa**,**b**,**c**, respectively) and anthracene-9,10-dione 10-oxime esters (**V**); **B:** Derivatives holding 4-nitrophenyl and 9,10-anthraquinone as novel oxime substrates with Ar and alkyl ester conjugates (**VI** and **VII**, respectively).

We have a strong interest in studying the photodegradation of DNA using small molecules, such as diacylhydrazine-bridged anthranilic acids,[34] quinazolinones[35,36] and their metal complexes,[37] as well as quinazolines and transition metal complexes[38,39] or arylazosulfones.[40] Our studies on oxime carboxylic esters have identified pyridine and 4-nitrophenyl amidoximes as =N-OH containing templates that efficiently photocleave DNA, similar to their aldoximes and ketoxime analogues.[18,19] Interestingly, oxime sulfonic alkyl and aryl ester conjugates were more photoreactive towards DNA than their related carboxylates.[41,42] Notably, oxime carbamate esters exhibited total chemoselectivity, with *p*-Cl-Ph carbamates (and, to a lesser extent, other halogenated derivatives) being the only active compounds.[43,44] One of these derivatives demonstrated insecticidal activity specifically in adult insect populations under controlled pesticide activation driven by UV-A irradiation.[44]

Although DNA-binding, photocleavage, and protein binding (Bovine and Human Serum Albumin, BSA and HSA, respectively) induced by small molecules are frequently reported in publications of this kind, protein photocleavage has been much less studied. One approach involves molecules containing photocleavable linkers, such as the nitrobenzyl group,[45] which, upon light exposure, provide a "turn on-off" mechanism for protein degradation through the release of active drugs.[46,47] Another approach utilizes photosensitizers that bind to specific protein sites and, upon light irradiation, cleave the proteins at those sites.[48,49] Identified photocleaving small molecules have also been incorporated into hybrids with larger species, serving as specialized photosensitizing agents. Significant work in the field has focused on substrates such as 2-hydroxy-1-naphthoic acids,[50] 2-phenylquinolines,[51–53] anthracenes,[54,55] pyrenes,[56–58] and both natural[59] and synthetic antraquinones.[54,60–64]

It appears that the potential of oxime ester substrates for DNA photocleavage might also be applicable to protein photodegradation. To the best of our knowledge, no oxime ester has been used in such experiments to date. Therefore, we have designed novel derivatives based on the photoactive substrates 4-nitro-benzaldehyde and 9,10-anthraquinone (Figure 2B, **VI** and **VII**, respectively). These derivatives, in addition to aromatic ester conjugates, incorporate alkyl moieties that generate stable alkyl radicals during the homolysis of the N-O bond and subsequent decarboxylation. This manuscript discusses their synthesis, DNA-binding and photocleavage properties, as well as their BSA- and HSA-binding and photocleavage activities.

Results and Discussion

Synthesis

For the new oxime scaffolds (4-nitrophenyl and 9,10-anthraquinone-2-), along with the aromatic ester frameworks, the design incorporated two novel residues: the isobutanoyl and the 2-phenyl-propanoyl groups. These were included to explore their reactivity. It is expected that, in contrast to alkyl ester residues, which do not photocleave DNA due to possible decarboxylation,[17,19] the aforementioned groups may facilitate the formation of the oxygen-centered radicals (**IXa** and **Xa**) upon irradiation. Possible decarboxylation is anticipated to generate secondary carbon-centered radicals (**IXb** and **Xb**; Figure 3A and 3B, respectively) with **Xb** further stabilized through resonance forms.

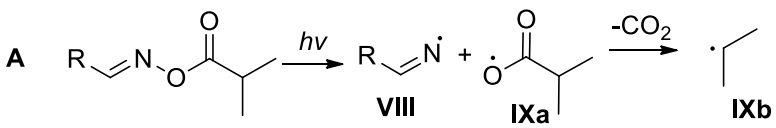

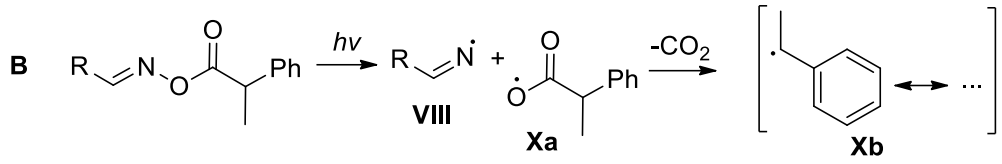

Figure 3. The isobutanoyl and the 2-phenyl-propanoyl groups.

Commercially available 4-nitrobenzaldehyde (**1**) has been treated with hydroxylamine hydrochloride (**2**), to give aldoxime (**3**) in 91% yield. The corresponding aldoxime has been employed under inert atmosphere in reaction with acyl halides **4** and triethylamine to produce oxime esters **5a-c** in good yields. Due to the sensitivity of **3**, the reaction with *p*-nitrobenzoyl chloride was not successful, on the contrary to its related 4-nitrobenzamidoxime.[18]

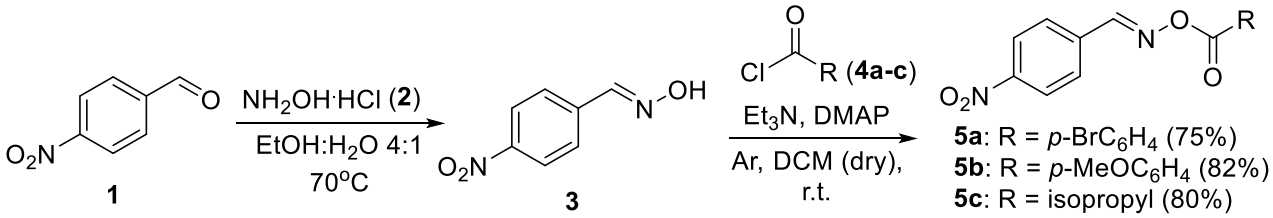

Scheme 1. Synthesis of aldoxime **3** and oxime esters **5a-c**.

For the synthesis of compound **5d** (Scheme 2), the use of 2-phenylpropanoic acid (**4d**) which was commercially available was found more suitable. Its transformation to a reactive form with coupling reagents (EDC[65–67] and DCC[68–70]) and optimization of the reaction conditions led to the use of DCC, DMAP in anhydrous DCM under argon for this particular reaction.

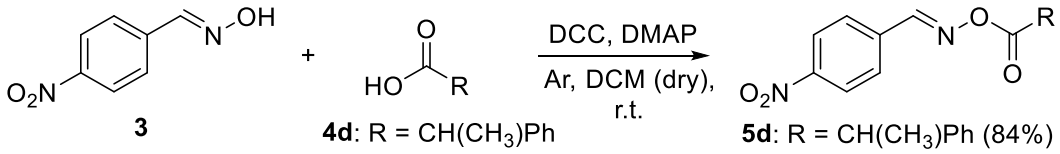

Scheme 2. Synthesis of **5d** with coupling reagent DCC.

Contrary to 4-nitrobenzalhyde which was rather straightforward to use and could easily produce most of the esters when paired with halides and acid, the formation of anthraquinone-2-carbaldehyde (**7**) was rather troublesome. The initial thought was to obtain **7** through the corresponding alcohol using oxidation protocols which in turn could be derived from 2-methylanthraquinone (**6**) after halogenation[71] and nucleophilic substitution to the bromine holding carbon. However, attempting to synthesize the bromide intermediate using radical reactions under reflux conditions, a mixture of three distinct products (most probably mono-, di-, and trisubstituted bromo-derivatives) has been produced, where neither the mono- or the di-bromo derivative[72] could be isolated. Attempts to produce **7** directly from oxidation of **6** using IBX as an oxidizing agent[73] and microwave irradiation were found to be unsuccessful to this substrate. Finally, in an effort to get intermediate **7**, SeO_2 has been used in order for the benzylic methyl group[74,75] of 2-methylanthraquinone to be oxidized. Indeed, those attempts using H_2SO_4 and heating the mixture for 5 min at 185 °C provided **7** in low

yields (25-42%). However, the starting material **6** was recovering and upon recycling and laboring column chromatography separations an efficient amount of **7** has been obtained (Scheme 3). The desired aldoxime **8**[76] was easily formed using hydroxylamine hydrochloride and K_2CO_3 in EtOH.

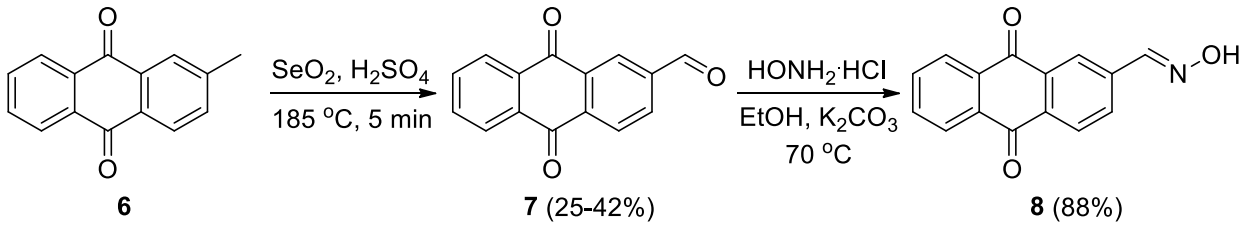

Scheme 3. Two step synthesis of aldoxime **8**.

In continuation, using the same acid halides and acid as with **3**, formation of **9a** in good yield has been realized (Scheme 4). Treatment of aldoxime **8** individually with **4c** and **4d** gave a mixture of two products where in each case one of them was in greater yield. However, separation of the main product either by column chromatography or by recrystallization was not possible, as the product seemed to decompose inside the column or not to crystallize.

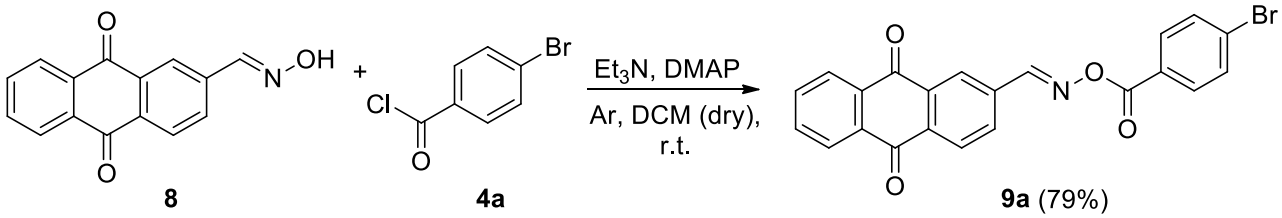

Scheme 4. Synthesis of 9,10-dioxo-9,10-dihydroanthracene-2-carbaldehyde *O*-(4-bromobenzoyl) oxime **9a**.

Having at hand a group of derivatives bearing the *p*-nitrophenyl chromophore with a variation of ester substituents (compounds **5a-d**) and one derivative with a planar anthraquinone photosensitive substrate **9a** closely related to **5a** (NMR spectra, Supplementary Material (SM): Figures S1-S12) we proceeded to the interactions and photocleavage experiments of DNA, BSA and HSA.

Affinity studies with calf-thymus DNA

The interaction between calf-thymus (CT) DNA and the oxime esters **5a-d** and **9a** has been studied using UV-vis spectroscopy, viscometry experiments and competitive studies with ethidium bromide (EB).

In the UV-vis spectra of compounds **5a-d** and **9a**, one (for **5a-d**) or two (for **9a**) bands appeared in the range 319-350 nm. The addition of incremental amounts of CT DNA into a DMSO solution of compounds **5a-d** and **9a** (Supplementary Material, Figure S13) resulted in hyperchromism or hypochromism of these bands accompanied by a slight (of 1 nm) blue- or red-shift (Table 1) illustrating their interaction with CT DNA. The Wolfe-Shimer equation[77] and the corresponding plots [DNA]/(ε_A–ε_f) *versus* [DNA] (Supplementary Material, Figure S14) were employed in order to determine the DNA-binding constants (Kb) of the compounds as shown in Table 1. The K_b values of the compounds are of the 10^6 M^{-1} magnitude, suggesting their tight interaction with CT DNA.

Table 1. UV–vis spectroscopic features from the interaction of compounds **5a-d** and **9a** with CT DNA. UV-band (λ_{max}, nm) (percentage of the observed hyper-/hypo-chromism ($\Delta A/A_0$, %), blue-/red-shift of the λ_{max} ($\Delta\lambda$, nm)), and DNA-binding constants (K_b, in M^{-1}).

Oxime ester	λ_{max} (nm) ($\Delta A/A_0$ (%) [a], $\Delta\lambda$ (nm))	K_b (M^{-1})
5a	325 (+24 [a], 0)	$2.30(\pm0.06)\times10^6$
5b	327 (+17, 0)	$3.09(\pm0.08)\times10^6$
5c	319 (+9, -1 [b])	$7.14(\pm0.10)\times10^6$
5d	320 (-23 [a], +1 [b])	$5.27(\pm0.06)\times10^6$
9a	329 (-14, 0), 350 (-12, +1)	$5.53(\pm0.05)\times10^6$

[a] "+" denotes hyperchromism, "-" denotes hypochromism;
[b] "+" denotes red-shift, "-" denotes blue-shift;

In an endeavor to shed light into the interaction mode of the compounds with CT DNA, the changes of the relative viscosity of a solution of CT DNA (0.1 mM) were monitored in the presence of increasing amounts of aldoxime esters **5a-d**, **9a** (up to the value of *r* = 0.27, Figure 4, SM: B2). More specifically, non-classical intercalation (groove-binding or electrostatic interactions) can be attributed to a stable or slightly decreased viscosity of the solution due to partial bending of DNA helix, while an intercalative mechanism is suggested upon increase of viscosity due to the lengthening of distance between base pairs at the binding region and the lengthening of the biomolecule.[78–80] Based on the changes of DNA-viscosity observed for compounds **5a-d**, initially (i.e. at low concentrations and up to r = [compound]/[DNA] = 0.1) the relative viscosity decreases or remains practically stable revealing an external interaction with CT DNA (probably groove-binding) whereas upon higher concentrations, the increase of relative viscosity is due to an intercalation mechanism (Figure 4). On the other hand, the anthraquinone derivative **9a** (Figure 4) appears to be the only one to interact exclusively through intercalation with DNA obviously via its extended planar tricyclic aromatic system.

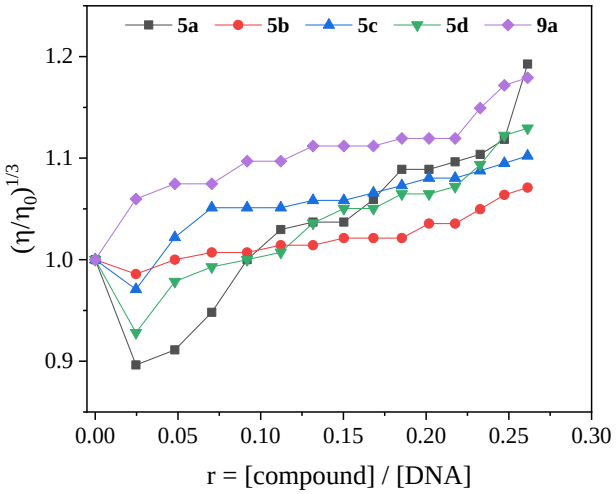

Figure 4. Relative viscosity $(\eta/\eta_0)^{1/3}$ of CT-DNA (0.1 mM) in buffer solution (150 mM NaCl and 15 mM trisodium citrate at pH 7.0) in the presence of increasing amounts of compounds **5a-d** and **9a** (*r* = [compound]/[DNA] = 0-0.27).

EB is a useful indicator of intercalation since it is a fluorescent compound and, when bound with linear DNA, presents an intense emission band at 592-593 nm (upon excitation at 540 nm) attributed to the insertion

of its phenanthridine group in-between the bases of DNA. A compound that is antagonistic to EB for the DNA-intercalation sites can induce a quenching of this emission band. Since the DNA-binding constants of compounds **5a-d** and **9a** are higher than that of ethidium bromide (EB) ($1.23(\pm0.07)\times10^5$ M^{-1})[81], the compounds may afford the displacement of the EB as a result of their DNA-intercalative potency. To study EB-displacing ability of compounds **5a-d** and **9a**, the changes in the fluorescence emission spectra of EB-DNA solution upon addition of compounds **5a-d** and **9a** are depicted in Figures 5(A) and S15 (Supplementary Material).

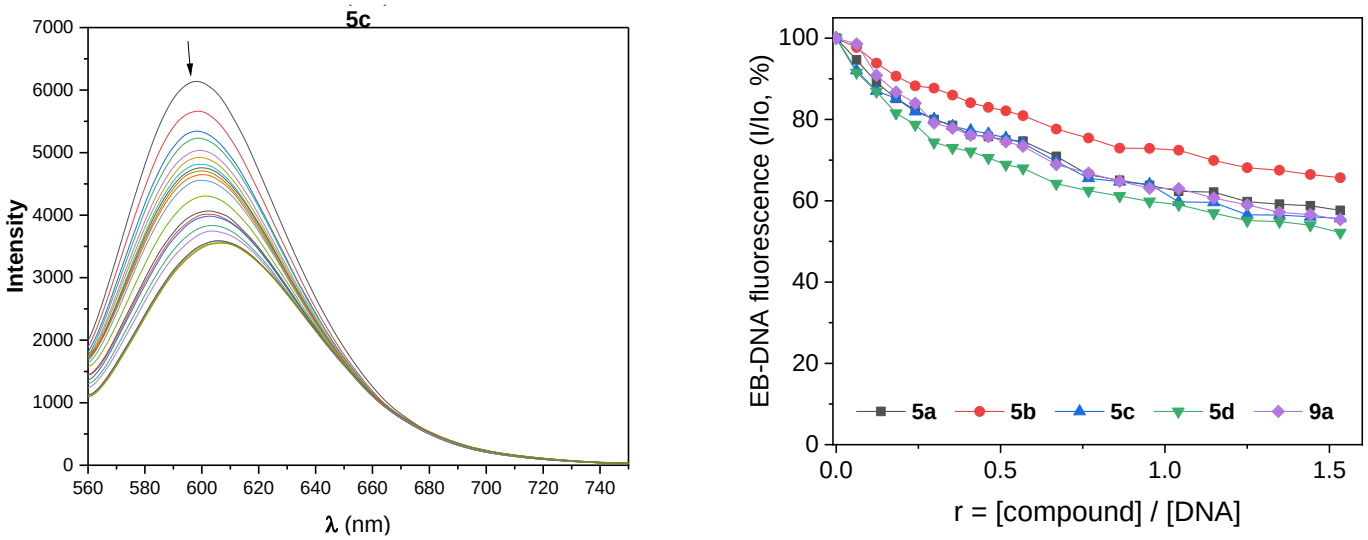

(A) (B)

Figure 5. (A) Fluorescence emission spectra ($\lambda_{excitation}$ = 540 nm) for EB–DNA ([EB] = 40 μM, [DNA] = 45 μM) in buffer solution (150 mM NaCl and 15 mM trisodium citrate at pH 7.0) in the absence and presence of increasing amounts of compound **5c**. The arrow shows the changes of intensity upon increasing amounts of the compound. (B) Plot of relative EB–DNA fluorescence intensity at $\lambda_{emission}$ = 592 nm (I/Io, %) *versus* r (*r* = [compound]/[DNA]) in the presence of compounds **5a-d** and **9a** (up to 57.7% of the initial EB–DNA fluorescence emission intensity for **5a**, 65.7% for **5b**, 55.6% for **5c**, 52.2% for **5d**, and 55.4% for **9a**).

As shown in Figure 5(B) and Table 2, a significant quenching of the EB-DNA band was observed (up to 47.8% for compound **5d**). The Stern-Volmer constants (K_{SV}) were calculated with Stern-Volmer equation (Equation S2)[82] and plots (Figure S16) and attest to a medium affinity for CT DNA. Finally, the EB-DNA quenching constants (k_q) were calculated with equation S3 (lifetime of EB-DNA (τ_0) is 23 ns)[83]) and are higher than the value of 10^{10} $M^{-1}s^{-1}$, indicating that a static quenching mechanism[82] occurs through energy transfer between orbitals of each compound and the fluorophore and confirming thus the interaction of the compounds with EB-DNA.

Table 2. Fluorescence features of the EB–displacement studies for compounds **5a-d** and **9a**: Percentage of EB-DNA fluorescence quenching (ΔI/Io, in %), Stern–Volmer constants (K_{SV}, in M^{-1}) and quenching constants of the EB–DNA fluorescence (k_q, in $M^{-1}s^{-1}$).

Oxime ester	$\Delta I/I_0$ (%)	K_{SV} (M^{-1})	k_q (M^{-1} s^{-1})
5a	42.3	$3.23(\pm0.11)\times10^3$	$1.40(\pm0.05)\times10^{11}$
5b	34.3	$2.10(\pm0.06)\times10^3$	$9.15(\pm0.25)\times10^{10}$

5c	44.4	$7.00(\pm0.18)\times10^{3}$	$3.04(\pm0.08)\times10^{11}$
5d	47.8	$1.33(\pm0.06)\times10^{4}$	$5.80(\pm0.25)\times10^{11}$
9a	44.6	$6.14(\pm0.22)\times10^{3}$	$2.79(\pm0.10)\times10^{11}$

Affinity studies with BSA and HSA

After the promising results derived from the CT DNA-affinity studies, we endeavored to examine if this could be repeated for bovine (BSA) and human serum albumin (HSA) as well. Serum albumins represent the highest protein fraction in plasma and serve various physiological roles. Importantly, serum albumins serve as carrier proteins for a wide range of compounds, such as fatty acids, hormones and drugs.[84] In addition, they share several features that make them suitable for drug delivery.[85] Both albumins are often utilized as models in studies and have many applications in recent years.[86–88]

The interactions between serum albumins and drugs/ligands have been studied via several methods.[89] Both BSA and HSA, when excited at 295 nm, display an fluorescence emission band with λ_{max} at 345 and 340 nm, respectively (SM: Section D1). The fluorescence emission spectra of the albumins (3 mM) in buffer solution were recorded in the range 300–500 nm for $\lambda_{excitation}$ = 295 nm upon incremental addition of the compounds (Figures S17 and S20). The presence of the compounds resulted in a moderate quenching of the albumin band which, on average, was more pronounced in the case of BSA (Figure 6). The inner–filter effect was also checked with equation S4,[90] and was found to be negligible to affect the measurements. The observed quenching is assigned to changes of the secondary structure of the albumins (re–arrangement or modifications) as a result from their interaction with the compounds.[82,91]

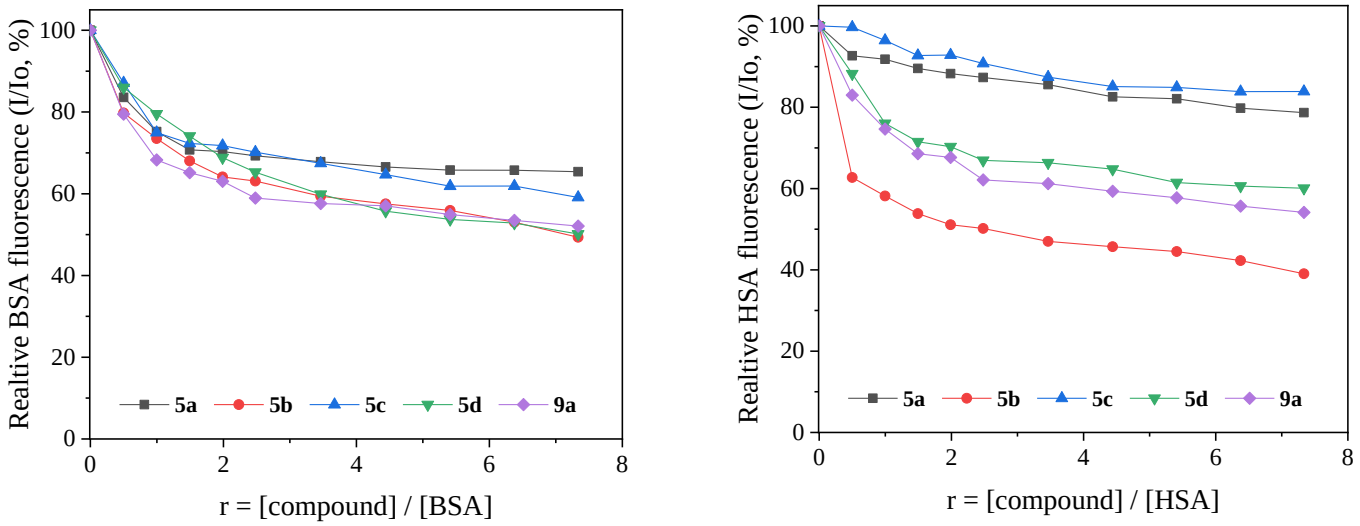

(A) (B)

Figure 6. (A) Plot of % relative BSA fluorescence emission intensity (I/Io, %) at $\lambda_{emission,max}$ = 345 nm *versus r* (= [compound]/[BSA]) for compounds **5a-d** and **9a** (up to 65.4% of the initial BSA fluorescence for **5a**, 49.4% for **5b**, 59.1% for **5c**, 50.2% for **5d**, and 52.1% for **9a**). (B) Plot of % relative HSA fluorescence emission intensity (I/Io %) at $\lambda_{emission,max}$ = 340 nm *versus r* (= [compound]/[HSA]) for compounds **5a-d** and **9a** (up to 78.7% of the initial HSA fluorescence for **5a**, 39.1% for **5b**, 83.9% for **5c**, 60.1% for **5d**, and 54.2% for **9a**).

The values of the corresponding K_{SV} and the k_q of the compounds for both albumins were calculated with the Stern–Volmer equations (equations S2 and S3) and the corresponding plots (Figures S18 and S21). All

calculated k_q values (Table 3) are higher than the value of 10^{10} $M^{-1}s^{-1}$ and confirm the interaction of the compounds with both albumins.[82]

Table 3. The albumin (HSA/BSA)–quenching constants (k_q), binding constants (K) and number of binding sites for compounds **5a-d** and **9a**.

Compound	$k_{q(BSA)}$ (M^{-1} s^{-1})	$K_{(BSA)}$ (M^{-1})	$n_{(BSA)}$	$k_{q(HSA)}$ (M^{-1} s^{-1})	$K_{(HSA)}$ (M^{-1})	$n_{(HSA)}$
5a	$9.20(\pm0.12)\times10^{12}$	$5.34(\pm0.15)\times10^{5}$	0.38	$9.46(\pm0.37)\times10^{11}$	$1.34(\pm0.16)\times10^{5}$	0.28
5b	$3.01(\pm0.18)\times10^{12}$	$3.58(\pm0.15)\times10^{5}$	0.52	$3.81(\pm0.27)\times10^{12}$	$7.75(\pm0.35)\times10^{5}$	0.59
5c	$1.84(\pm0.06)\times10^{12}$	$2.50(\pm0.12)\times10^{5}$	0.47	$1.35(\pm0.03)\times10^{12}$	$6.11(\pm0.09)\times10^{5}$	0.31
5d	$5.80(\pm0.34)\times10^{12}$	$1.54(\pm0.05)\times10^{5}$	0.65	$1.97(\pm0.15)\times10^{12}$	$3.79(\pm0.19)\times10^{5}$	0.44
9a	$8.99(\pm0.11)\times10^{12}$	$4.49(\pm0.21)\times10^{5}$	0.52	$6.37(\pm0.08)\times10^{12}$	$3.35(\pm0.14)\times10^{5}$	0.51

The albumin–binding constants (K) of the compounds were determined with the Scatchard equation (equation S5) and the corresponding plots (Figures S19 and S22). Compounds **5a** and **5b** present the highest BSA-binding ($K_{BSA,\mathbf{5a}}$ = $5.34(\pm0.15)\times10^{5}$ M^{-1}) and HSA-binding constants ($K_{HSA,\mathbf{5b}}$ = $7.75(\pm0.35)\times10^{5}$ M^{-1}), respectively, among the compounds (Table 3). The K values of the compounds (Table 3) are relatively high, of the magnitude 10^5 M^{-1}, and indicate a rather tight and reversible binding to albumins (having the ability to get released at the potential targets), when compared to the strongest non–covalent interactions which have a binding constant of 10^{15} M^{-1}.[92]

Photocleavage activity studies

The purpose of such studies is multifaceted; in general, any alteration to DNA or proteins can point to possible anti-tumor or anti-microbial activity, respectively. Furthermore, photocleavage of such proteins can be exploited to study their interactions with small molecules, participate in SAR studies or even develop novel drugs through docking studies. Our photocleavage studies were carried on with a UV-A lamp (365 nm, broadband lamp) at 10 cm distance from our samples for 2 or 4 h (4 h is the case with albumins) and concentrations of the compounds determined by our findings as we saw fit. For all the sample solutions, DMSO and pBluescript KS II plasmid DNA (pDNA) were used.

All carboxylic oxime esters have been tested at 500 μM and exhibited great photocleavage activity with the highest being attributed to **9a** (up to 96%), next being **5a** (57%) (Figure 7). Evidently, the hypothesis of the possible reactivity of both isobutanoyl and the 2-phenyl-propanoyl conjugates on derivatives **5c** and **5d** turned out to be a plausible scenario, since those derivatives appeared to have similar photocleavage activity with an aryloyl derivative **5b**.

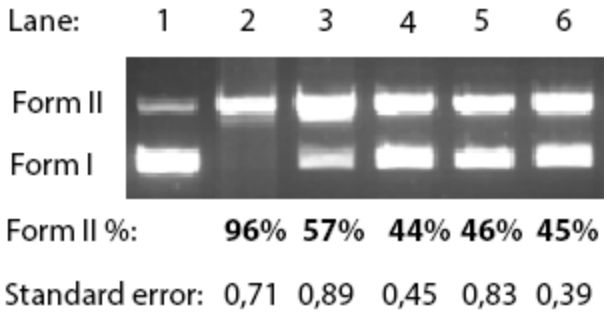

Figure 7. pDNA photocleavage with UV-A irradiation (365nm) for 1h. From left to right: control DNA, neat, irradiated (lane 1); lanes 2-6: DNA solution at 500μM with esters **9a**, **5a**, **5c**, **5d** and **5b**, respectively.

As for derivatives **5b-d** the cleavage of pDNA appeared below 50%, the focus turned to the effective concentration where compounds **9a** and **5a** would cause damage up to 50% of the supercoiled pDNA. The photocleavage activity at both 250 μM and 100 μM for **9a** turned out to be 85% and 80%, respectively (formation of nicked pDNA, Form II, Figure 8A, lanes 2 and 3), while for compound **5a** it dropped to 39% and 25% (Figure 8A, lane 4 and Figure 8B, lane 5, respectively). It appeared that **9a** has been efficiently photocleaving pDNA with an effective concentration as low as 50 μM (Figure 8B, lane 2). The obvious superiority of **9a** is most probably attributed to the flatness of the tricyclic system of anthraquinone that provides better intercalation to pDNA.

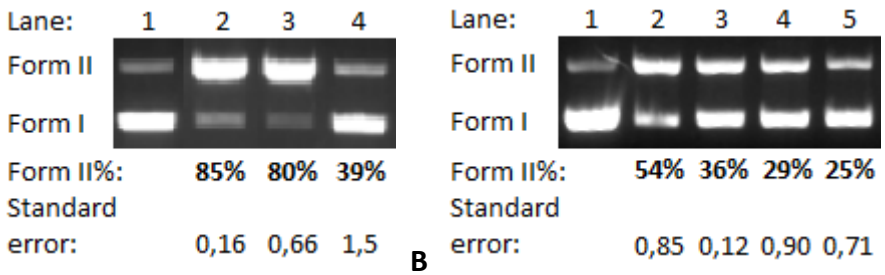

Figure 8A and 8B. pDNA photocleavage with UV-A irradiation (365 nm) for 1 h. Figure 8A: from left to right: control DNA, neat, irradiated (lane 1); lanes 2-3: DNA with **9a** at concentration 250 and 100 μM, respectively;

lane 4: DNA with **5a** (250 μM). Figure 8B: from left to right: control DNA, neat, irradiated (lane 1); lanes 2-4: DNA with **9a** at concentration 50, 25 and 10 μM, respectively; lane 5: DNA with **5a** (100 μM).

The photocleavage activity of all esters on BSA and HSA has also been examined. As far as BSA is concerned, the presence of protein fragments almost in every tested compound has been evidenced through gel electrophoresis, upon irradiation at 365 nm for 2 h. *p*-Nitro-benzoyl derivative **5a** showed better photocleavage activity than its corresponding *p*-MeO-benzoyl derivative **5b** (Figure 9A). Interestingly, the isobutanoyl derivative **5c** showed a photodigestion which seemed to be in reverse analogy to its concentration, as the new fragments which appear in Figure 9A, **5c** progressively faint by decreasing the concentration from 500 to 400, 300, 200 and 100 μM (Figure 9A, lanes 3-7, respectively). In all experiments and in the lack of a compound, both BSA and HSA controls non-irradiated and irradiated samples seemed to be the same (Figure 9A and 9B: lane 1: non-irradiated; lane 2: irradiated).

Comparing the two aroyl derivatives **5a** and **5b**, **5a** seemed to be more powerful, whereas **5b** and **5d** were not harmful to BSA. The anthraquinone derivative **9a**, however, was superior to all (Figure 9A), similarly to the case with the pDNA photocleavage, Figure 8. Interestingly, HSA seemed to be more photosensitive, and all new photosensitizers **5a-d** and **9a** photocleaved the protein. The reverse analogy to the concentration is evidenced at the gels with the lowest concentration of 100 μM to cause the less damage (Figure 9B, lane 7).

The encouraging results prompted us to exhaustingly irradiate the two best compounds **5a** and **9a** with the proteins for a 4 h period (Figure 10). These harsh conditions showed that the damage was analogous to the irradiation time. Checking lane 3, **5a** (Figure 9), and the respective lane 3, **5a** (Figure 10), it is more than obvious that without changing the concentration (500 μM) the damage caused in 2 h and 4 h is in favor of the prolonged time irradiation. The same is obvious for the rest of the concentrations. Nevertheless, the effect was less pronounced at lower concentrations.

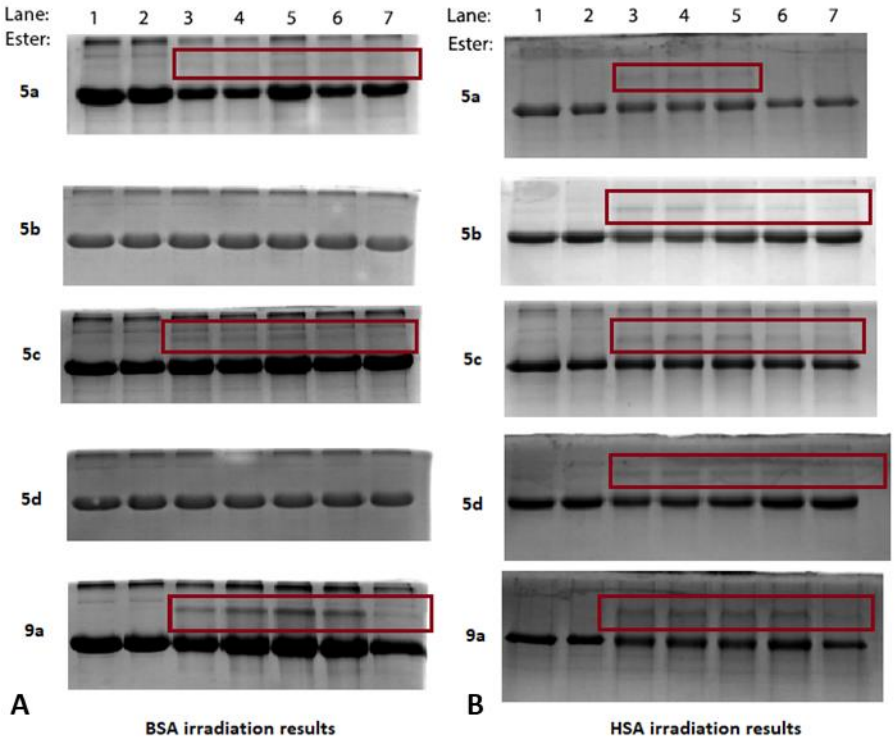

Figure 9. Irradiation of BSA (left) and HSA (right) solution in the presence of esters **5a-d**, **9a** for 2 h. In every case lane 1 and lane 2 are control samples, the first being irradiated albumin solution in the absence of ester,

lane 2 was non-irradiated albumin solution with DMSO, lanes 3, 4, 5, 6 and 7 are irradiated albumin solution with each ester at concentration 500 μM, 400 μM, 300 μM, 200 μM, 100 μM, respectively.

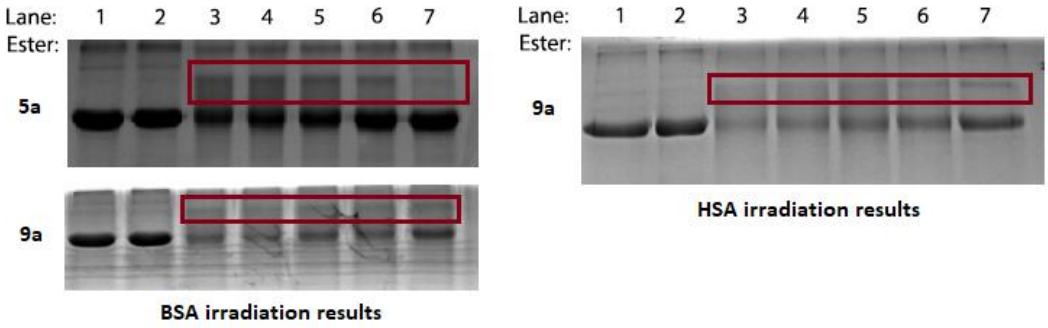

Figure 10. Irradiation of BSA (left) and HSA (right) solution in the presence of esters **5a** and or **9a** for 4 h. In every case lane 1 and lane 2 are control samples, the first being irradiated albumin solution in the absence of ester, lane 2 was non-irradiated albumin solution with DMSO, lanes 3, 4, 5, 6 and 7 are irradiated albumin solution with each ester at concentration 500 μM, 400 μM, 300 μM, 200 μM, 100 μM, respectively.

Once again, the best photosensitizer, derivative **9a**, had an impressive impact on BSA in all concentrations showing reverse analogy to the concentration and analogy to the irradiation time (Figure 10, left, picture **9a**). In the case of HSA, anthraquinone **9a** was further examined in a 4 h irradiation protocol, where the cleavage effect was more pronounced than BSA. Based on these results, the stronger effect on the higher molecular fraction and the non-visible molecular weight fragment is speculated to be rather of non-specific binding/cleavage.

Conclusions

Novel oxime esters based on 4-nitrobenzaldehyde and 9,10-anthraquinone-2-carboxaldehyde templates have been synthesized. Specifically, the monocyclic aromatic aldoxime **3** was conjugated with two aromatic and two aliphatic carboxylic residues to yield derivatives **5a-d**. The isobutanoyl and 2-phenylpropanoyl moieties were selected as ester conjugates to provide stable aliphatic or benzylic type radicals upon possible decarboxylation. Additionally, 9,10-anthraquinone-2-carboxamidoxime **8** was transformed into its *p*-Br-phenyl ester **9a**.

All five tested compounds exhibited strong interactions with CT DNA. Compounds **5a-d** demonstrated an initial groove-binding interaction followed by intercalation with CT DNA, while compound **9a** interacted exclusively through intercalation of its planar aromatic anthraquinone system between DNA bases. Furthermore, the compounds showed tight and reversible interactions with BSA and HSA, indicating their potential for transport to biological targets.

Among the four derivatives **5a-d**, the *p*-nitrobenzoyl derivative **5a** displayed superior DNA-photocleavage activity, while the aliphatic derivatives **5c** and **5d** exhibited activity similar to the *p*-MeO-benzoyl compound **5b**. Compounds **5a** and **5c** caused BSA-photodegradation, and all 4-nitrobenzaldehyde oxime esters **5a-d** photocleaved HSA upon irradiation at 365 nm. The tricyclic, planar anthraquinone scaffold with an oxime ester at position 2, **9a**, served as the basis for comparison with its relative **5a**. Anthraquinone derivatives consistently demonstrated superior activity in DNA, BSA and HSA photocleavage experiments. Notably, **9a**

photocleaved pDNA at a concentration of 50 μM, while **5a** required concentrations >250 μM. Similarly, **9a** exhibited stronger BSA-photodegradation activity. In all experiments, BSA was more resistant than HSA, with anthraquinone completely fragmenting HSA after four hours of irradiation at 365 nm.

These findings highlight 4-nitrobenzaldehyde and 9,10-anthraquinone-2-carboxaldehyde oxime esters as novel photosensitizers, positioning them as promising lead compounds for photobiological applications in cancer treatment and microbial photo-inactivation studies.

Experimental Section

General. All reagents including raw materials were commercially available and used without further purification. The ^{1}H NMR and ^{13}C NMR spectra were recorded with Agilent 500 (^{1}H: 500 MHz, ^{13}C: 126 MHz), obtained at room temperature using either $CDCl_3$ or DMSO-d_6 as solvent and analyzed with the software MestReNova (see Supplementary Material, Figures S1-S12). FTIR analysis was performed using an IROS 05 FTIR spectrometer (Ostec Enterprise Ltd, Moscow, Russia) equipped with ATR (Attenuated Total Reflectance) crystal or Thermo Scientific Nicolet iS20 FT–IR ATR spectrometer in the range 400–4000 cm^{-1}. Irradiation protocols were executed with a UV-A lamp distanced 10 cm from the samples. Gel electrophoresis experiments were performed using 1% agarose and 15% polyacrylamide while the CT DNA used was pBluescript KS II. Gels were analyzed under visible light with MiniBIS Pro.

Study of the biological profile of the compounds. All the procedures and relevant equations used in the *in vitro* study of the biological activity (interaction with CT DNA, plasmid DNA, HSA and BSA) of the compounds can be found in the Supplementary Material (Sections B-C). DNA and BSA-HSA photocleavage SM: Section D-E.

Synthesis. Reaction progress was monitored using TLC chromatography and during every reaction, a magnetic stirrer was used at all times. Removal of excess solvent was achieved through a rotary evaporation instrument under reduced pressure.

4-Nitrobenzaldehyde *O*-(4-bromobenzoyl) oxime (5a). Under inert atmosphere, 4-nitrobenzaldehyde oxime **3**[18] (100 mg, 1 eq.) is added in a round-bottom flask, anhydrous DCM (25 mL), DMAP (0.05%), Et_3N (0.092 mL, 1.1 eq.) and 4-bromobenzoyl chloride (145 mg, 1.1 eq.) is transferred to the reaction mixture under stirring. After a 2 h timeline has elapsed, the crude product is extracted (3 × 50 mL) and after recrystallization (DCM/PS) yellow crystals, mp 170−171 °C, were obtained in 75% yield. IR (neat): 1740 cm^{-1}; ^{1}H NMR (500 MHz, $CDCl_3$, 25 ^{o}C): δ_H: 7.83 (d, *J* = 8.5 Hz, 2H), 8.00 (d, *J* = 8.5 Hz, 2H), 8.08 (d, *J* = 8.9 Hz, 2H), 8.37 (d, *J* = 8.9 Hz, 2H), 9.11 (s, 1H); ^{13}C NMR (125 MHz, DMSO-d_6, 25 ^{o}C): δ_C: 124.3, 127.0, 128.2, 129.5, 131.3, 132.2, 136.1, 149.2, 156.7, 162.3; HRMS (ESI) *m/z* [2M+Na]$^{+}$: $C_{28}H_{18}Br_2N_4NaO_8^{+}$, calc: 718.9384; found: 718.9378.

4-Nitrobenzaldehyde *O*-(4-methoxybenzoyl) oxime (5b). Under inert conditions through the use of argon balloon, 4-nitrobenzaldehyde oxime (100 mg, 1 eq.), anhydrous DCM (25 mL), DMAP (0.05%), Et_3N (0.092 mL, 1.1 eq.) and 4-methoxybenzoyl chloride (113 mg, 1.1 eq.) is transferred to a round-bottom flask under stirring. After 4 h, the reaction mixture is subjected to extraction (3 × 50 mL) and after recrystallization (DCM/PS) pale yellow crystals, mp 180−183 °C, were obtained in 82% yield. IR (neat): 1730 cm^{-1}; ^{1}H NMR (500 MHz, $CDCl_3$, 25 ^{o}C): δ_H: 3.87 (s, 3H), 7.12 (d, *J* = 8.9 Hz, 2H), 8.03 (d, *J* = 8.8 Hz, 2H), 8.07 (d, *J* = 8.8 Hz, 2H), 8.36 (d, *J* = 8.9 Hz, 2H), 9.06 (s, 1H); ^{13}C NMR (125 MHz, DMSO-d_6, 25 ^{o}C), δ_C: 55.7, 114.5, 119.7, 124.3, 129.4, 131.7, 136.4, 149.1, 156.0, 162.1, 163.8; HRMS (ESI) *m/z* [2M+Na]$^{+}$: $C_{30}H_{24}N_4NaO_{10}^{+}$, calc: 623.1385; found: 623.1389.

4-Nitrobenzaldehyde *O*-isobutanoyl oxime (5c). Under inert conditions, 4-nitrobenzaldehyde oxime (180 mg, 1 eq.), anhydrous DCM (25 mL), DMAP (0.05%), Et_3N (0.092 mL, 1.1 eq.) is added to the reaction mixture. Isobutanoyl chloride (0.125 mL, 1.1 eq.) is transferred dropwise and under stirring. By the end of 3 h, the crude product is extracted (3 × 50 mL) and recrystallized (DCM/PS) to give colorless crystals, mp 138−140 °C, 80% yield. IR (neat): 1756 cm^{-1}; ^1H NMR (500 MHz, $CDCl_3$, 25 °C): δ_H: 1.19 (d, *J* = 7.0 Hz, 6H), 2.76 (hept, *J* = 6.9 Hz, 1H), 8.02 (d, *J* = 8.8 Hz, 2H), 8.33 (d, *J* = 8.8 Hz, 2H), 8.67 (s, 1H); ^{13}C NMR (125 MHz, DMSO-d_6, 25 °C): δ_C: 18.7, 32.0, 124.2, 129.4, 136.4, 149.1, 155.5, 173.4; HRMS (ESI) *m/z* $[M+Na]^+$: $C_{11}H_{12}N_2NaO_4^+$, calc: 259.0689; found: 259.0698.

4-Nitrobenzaldehyde *O*-(2-phenylpropanoyl) oxime (5d). Under inert atmosphere, anhydrous DCM (25 mL), DCC (422 mg, 2 eq.), DMAP (0.05%) and 2-phenylpropanoic acid (0.28 mL, 2 eq.) is added in dropwise motion. After 1.5 h, 4-nitrobenzaldehyde oxime (180 mg, 1 eq.) is added as well. The reaction mixture is subjected to extraction (3 × 50 mL) and recrystallization to isolate colorless crystals, mp 168−170 °C, in 84% yield. IR (neat): 1756 cm^{-1}; ^1H NMR (500 MHz, $CDCl_3$, 25 °C): δ_H: 1.49 (d, *J* = 7.1 Hz, 3H), 4.04 (q, *J* = 7.1 Hz, 1H), 7.35-7.38 (m, 5H), 8.00 (d, *J* = 8.8 Hz, 2H), 8.32 (d, *J* = 8.9 Hz, 2H), 8.82 (s, 1H); ^{13}C NMR (125 MHz, DMSO-d_6, 25 °C): δ_C: 18.5, 43.2, 124.1, 127.3, 127.4, 128.8, 129.4, 136.2, 139.9, 149.1, 155.7, 171.0; HRMS (ESI) *m/z*: Could not be found under the ESI conditions.

9,10-Dioxo-9,10-dihydroanthracene-2-carbaldehyde (7). Contrary to the method presented in literature where a photochemical process is preferred,[93] our procedure involved the addition of SeO_2 (333 mg, 3 eq.) and H_2SO_4 (0.45 mL) in a pear-shaped flask under mild stirring. 2-Methyl anthraquinone (222 mg, 1 eq.) was added and the mixture is heated at 185 °C for 5 min with an oil bath. The excess of acid is neutralized with Na_2CO_3 and the reaction mixture is filtered through celite to remove inorganic compounds and wash with EA. Drying the crude product with Na_2SO_4, separation with column chromatography and condensation leads to a yellow product in 25-42% yield. The material was used crude at the next step. ^1H NMR (500 MHz, $CDCl_3$, 25 °C): δ_H: 7.84-7.89 (m, 2H), 8.31 (dd, *J* = 8.0, 1.6 Hz, 1H), 8.32-8.40 (m, 2H), 8.49 (d, *J* = 8.0 Hz, 1H), 8.80 (d, *J* = 1.7 Hz, 1H), 10.25 (s, 1H).

9,10-Dioxo-9,10-dihydroanthracene-2-carbaldehyde oxime (8). In a manner similar to the one described in literature[94] the synthesis is conducted in a round-bottom flask where 9,10-dioxo-9,10-dihydroanthracene-2-carbaldehyde (50 mg, 1 eq.), K_2CO_3 (43 mg, 1.5 eq.) is added along with hydroxylamine hydrochloride (22 mg, 1.5 eq.) in CH_3CH_2OH:H_2O = 4:1 under reflux conditions at 70 °C for 2 h. The reaction mixture is concentrated in vacuo, extracted (3 × 200 mL) to get a yellow solid in 88% yield. ^1H NMR (500 MHz, $CDCl_3$, 25 °C): δ_H: 7.93-7.96 (m, 2H), 8.12 (dd, *J* = 8.1, 1.7 Hz, 1H), 8.20-8.24 (m, 3H), 8.41 (brs, 2H), 11.84 (s, 1H).

9,10-Dioxo-9,10-dihydroanthracene-2-carbaldehyde *O*-(4-bromobenzoyl) oxime (9a). The aldoxime is transferred to a round-bottom flask and is azeotropically dried with toluene. Then anhydrous DCM is added (10 mL) along with DMAP (0.05%) and Et_3N (0.085 mL, 1.1 eq.) under inert conditions. 4-bromobenzoyl chloride (48 mg, 1.1 eq.) is added under stirring and after 30 min, the mixture is extracted with DCM (3 × 50 mL), condensed and washed with EA to procure a bright green solid, mp 200−201 °C, in 79% yield. IR (neat): 1741 cm^{-1}; ^1H NMR (500 MHz, $CDCl_3$, 25 °C): δ_H: 7.66 (d, *J* = 8.5 Hz, 2H), 7.80-7.88 (m, 2H), 8.01 (d, *J* = 8.5 Hz, 2H), 8.32-8.36 (m, 2H), 8.38 (dd, *J* = 8.1, 1.6 Hz, 1H), 8.41 (d, *J* = 8.1 Hz, 1H), 8.59 (d, *J* = 1.6 Hz, 1H), 8.72 (s, 1H); ^{13}C NMR (125 MHz, DMSO-d_6, 25 °C): δ_C: 127.5, 127.8, 128.5, 128.5, 129.4, 131.7, 132.5, 132.8, 133.7, 133.8, 134.4, 134.9, 134.9, 135.7, 135.9, 155.6, 163.3, 182.7, 182.8; HRMS (ESI) *m/z* $[M+Na]^+$: $C_{22}H_{12}BrNNaO_4^+$, calc: 455.9842; found: 455.9842.

Acknowledgements

The authors acknowledge Maroula G. Kokotou, Laboratory of Chemistry, Department of Food Science and Human Nutrition, Agricultural University of Athens, for the HRMS analysis.

Supplementary Material

All the plots concerning affinity studies with DNA, BSA and HSA that were not presented in the main article along with the NMR spectra of the synthesized compounds and the irradiation protocols used are described in the Supplementary Material.

References

1. Singh, J.; Castle, S. L. *Arkivoc* **2024**, *2*, 202312065. https://doi.org/10.24820/ark.5550190.p012.065
2. Liu, L.; Duan, X. H.; Guo, L. N. *Synthesis* **2021**, *53*, 4375. https://doi.org/10.1055/a-1545-6874
3. Jackman, M. M.; Cai, Y.; Castle, S. L. *Synthesis* **2017**, *49*, 1785. https://doi.org/10.1055/s-0036-1588707
4. Walton, J. C. *Molecules* **2016**, *21*, 660. https://doi.org/10.3390/molecules21050660
5. Balakhonov, R. Y.; Mekeda, I. S.; Shirinian, V. Z. *Adv. Synth. Catal.* **2023**, *365*, 3690. https://doi.org/10.1002/adsc.202300833
6. Dong, D. Q.; Song, J. C.; Yang, S. H.; Qin, Q. X.; Wang, Z. L.; Zhang, E. X.; Sun, Y. Y.; Han, Q. Q.; Yue, S. *Chin. Chem. Lett.* **2022**, *33*, 1199. https://doi.org/10.1016/j.cclet.2021.08.067
7. Rykaczewski, K. A.; Wearing, E. R.; Blackmun, D. E.; Schindler, C. S. *Nat. Synth.* **2022**, *1*, 24. https://doi.org/10.1038/s44160-021-00007-y
8. Zard, S. Z. *Arkivoc* **2024**, *2*, 202312112. https://doi.org/10.24820/ark.5550190.p012.112
9. Kalsoom, I.; Bilal, M.; Kanwal, A.; Rasool, N.; Nazeer, U.; Ciurea, C.; Elena Neculau, A.; Constantina Martinescu, C. *J. Saudi Chem. Soc.* **2024**, *28*, 101848. https://doi.org/10.1016/j.jscs.2024.101848
10. Zhong, L. J.; Fan, J. H.; Chen, P.; Huang, P. F.; Xiong, B. Q.; Tang, K. W.; Liu, Y. *Org. Biomol. Chem.* **2024**, *22*, 10. https://doi.org/10.1039/D3OB01762A
11. Xiao, T.; Huang, H.; Anand, D.; Zhou, L. *Synthesis* **2020**, *52*, 1585. https://doi.org/10.1055/s-0039-1690844
12. Yousefnejad, F.; Gholami, F.; Larijani, B.; Mahdavi, M. *Top. Curr. Chem*. **2023**, *381*, 17. https://doi.org/10.1007/s41061-023-00431-y
13. Jiang, H. M.; Zhao, Y. L.; Sun, Q.; Ouyang, X. H.; Li, J. H. *Molecules* **2023**, *28*, 1775. https://doi.org/10.3390/molecules28041775
14. Vessally, E.; Saeidian, H.; Hosseinian, A.; Edjlali, L.; Bekhradnia, A. *Curr. Org. Chem.* **2017**, *21*, 249.

https://doi.org/10.2174/1385272820666161018150925
15. Walton, J. C. *Molecules* **2016**, *21*, 63. https://doi.org/10.3390/molecules21010063
16. Hammoud, F.; Hijazi, A.; Schmitt, M.; Dumur, F.; Lalevée, J. *Eur. Polym. J.* **2023**, *188*, 111901. https://doi.org/10.1016/j.eurpolymj.2023.111901
17. Theodorakis, E. A.; Xiang, X.; Lee, M.; Gibson, T. *Tetrahedron Lett.* **1998**, *39*, 3383. https://doi.org/10.1016/S0040-4039(98)00509-7
18. Pasolli, M.; Dafnopoulos, K.; Andreou, N.-P.; Gritzapis, P. S.; Koffa, M.; Koumbis, A. E.; Psomas, G.; Fylaktakidou, K. C. *Molecules* **2016**, *21*, 864. https://doi.org/10.3390/molecules21070864
19. Karamtzioti, P.; Papastergiou, A.; Stefanakis, J. G.; Koumbis, A. E.; Anastasiou, I.; Koffa, M.; Fylaktakidou, K. C. *MedChemComm* **2015**, *6*, 719. https://doi.org/10.1039/C4MD00548A
20. Bindu, P. J.; Mahadevan, K. M.; Satyanarayan, N. D.; Ravikumar Naik, T. R. *Bioorg. Med. Chem. Lett.* **2012**, *22*, 898. https://doi.org/10.1016/j.bmcl.2011.12.037
21. Chowdhury, N.; Dutta, S.; Dasgupta, S.; Singh, N. D. P.; Baidya, M.; Ghosh, S. K. *Photochem. Photobiol. Sci.* **2012**, *11*, 1239. https://doi.org/10.1039/c2pp25033k
22. Hwu, J. R.; Tsay, S. C.; Hong, S. C.; Hsu, M. H.; Liu, C. F.; Chou, S. S. P. *Bioconjugate Chem.* **2013**, *24*, 1778. https://doi.org/10.1021/bc400060h
23. Chou, S. S. P.; Juan, J. C.; Tsay, S. C.; Huang, K. P.; Hwu, J. R. *Molecules* **2012**, *17*, 3370. https://doi.org/10.3390/molecules17033370
24. Hwu, J. R.; Tsay, S. C.; Hong, S. C.; Leu, Y. J.; Liu, C. F.; Chou, S. S. P. *Tetrahedron Lett.* **2003**, *44*, 2957. https://doi.org/10.1016/S0040-4039(03)00375-7
25. Hwu, J. R.; Yang, J. R.; Tsay, S. C.; Hsu, M. H.; Chen, Y. C.; Chou, S. S. P. *Tetrahedron Lett.* **2008**, *49*, 3312. https://doi.org/10.1016/j.tetlet.2008.03.056
26. Zhao, L.; Zheng, L. *Molecules* **2023**, *28*, 8139. https://doi.org/10.3390/molecules28248139
27. Rajendran, M. *Photodiagn. Photodyn. Ther.* **2016**, *13*, 175. https://doi.org/10.1016/j.pdpdt.2015.07.177
28. Chen, C. X.; Yang, S. S.; Pang, J. W.; He, L.; Zang, Y. N.; Ding, L.; Ren, N. Q.; Ding, J. *Environ. Sci. Ecotechnology* **2024**, *22*, 100449. https://doi.org/10.1016/j.ese.2024.100449
29. Mantareva, V.; Braikova, D.; Lazarova, I.; Genova, T. *Front. Biosci. -Landmark* **2024**, *29*, 168. https://doi.org/10.31083/j.fbl2905168
30. Nowak-Perlak, M.; Ziółkowski, P.; Woźniak, M. *Phytomedicine* **2023**, *119*, 155035. https://doi.org/10.1016/j.phymed.2023.155035
31. Alvarez, N.; Sevilla, A. *Int. J. Mol. Sci.* **2024**, *25*, 1023. https://doi.org/10.3390/ijms25021023
32. da Cruz Rodrigues, A.; Bilha, J. K.; Pereira, P. R. M.; de Souza, C. W. O.; Passarini, M. R. Z.; Uliana, M. P. *Braz. J. Microbiol.* **2024**, *55*, 1139. https://doi.org/10.1007/s42770-024-01278-1
33. Ryu, V.; Uknalis, J.; Corradini, M. G.; Chuesiang, P.; McLandsborough, L.; Ngo, H.; Jin, T.; Fan, X. *Foods* **2023**, *12*, 4195. https://doi.org/10.3390/foods12234195
34. Mitrakas, A.; Stathopoulou, M. K.; Mikra, C.; Konstantinou, C.; Rizos, S.; Malichetoudi, S.; Koumbis, A. E.;

Koffa, M.; Fylaktakidou, K. C. **2024**, *29*, 647.
https://doi.org/10.3390/molecules29030647
35. Mikra, C.; Bairaktari, M.; Petridi, M.-T.; Detsi, A.; Fylaktakidou, K. C. *Processes* **2022**, *10*, 384.
https://doi.org/10.3390/pr10020384
36. Panagopoulos, A.; Balalas, T.; Mitrakas, A.; Vrazas, V.; Katsani, K. R.; Koumbis, A. E.; Koukourakis, M. I.; Litinas, K. E.; Fylaktakidou, K. C. *Photochem. Photobiol.* **2021**, *97*, 826.
https://doi.org/10.1111/php.13376
37. Lazou, M.; Tarushi, A.; Gritzapis, P.; Psomas, G. *J. Inorg. Biochem.* **2020**, *206*, 111019.
https://doi.org/10.1016/j.jinorgbio.2020.111019
38. Kakoulidou, C.; Gritzapis, P. S.; Hatzidimitriou, A. G.; Fylaktakidou, K. C.; Psomas, G. *J. Inorg. Biochem.* **2020**, *211*, 111194.
https://doi.org/10.1016/j.jinorgbio.2020.111194
39. Kakoulidou, C.; Chasapis, C. T.; Hatzidimitriou, A. G.; Fylaktakidou, K. C.; Psomas, G. *Dalton Trans.* **2022**, *51*, 16688.
https://doi.org/10.1039/D2DT02622H
40. Mikra, C.; Mitrakas, A.; Ghizzani, V.; Katsani, K. R.; Koffa, M.; Koukourakis, M.; Psomas, G.; Protti, S.; Fagnoni, M.; Fylaktakidou, K. C. *Int. J. Mol. Sci.* **2023**, *24*, 1834.
https://doi.org/10.3390/ijms24031834
41. Andreou, N. P.; Dafnopoulos, K.; Tortopidis, C.; Koumbis, A. E.; Koffa, M.; Psomas, G.; Fylaktakidou, K. C. *J. Photochem. Photobiol. B Biol.* **2016**, *158*, 30.
https://doi.org/10.1016/j.jphotobiol.2016.02.017
42. Papastergiou, A.; Perontsis, S.; Gritzapis, P.; Koumbis, A. E.; Koffa, M.; Psomas, G.; Fylaktakidou, K. C. *Photochem. Photobiol. Sci.* **2016**, *15*, 351.
https://doi.org/10.1039/c5pp00439j
43. Gritzapis, P. S.; Varras, P. C.; Andreou, N. P.; Katsani, K. R.; Dafnopoulos, K.; Psomas, G.; Peitsinis, Z. V.; Koumbis, A. E.; Fylaktakidou, K. C. *Beilstein J. Org. Chem.* **2020**, *16*, 337.
https://doi.org/10.3762/bjoc.16.33
44. Panagopoulos, A.; Alipranti, K.; Mylona, K.; Paisidis, P.; Rizos, S.; Koumbis, A. E.; Roditakis, E.; Fylaktakidou, K. C. *DNA* **2023**, *3*, 85.
https://doi.org/10.3390/dna3020006
45. Fu, W.; Shao, Z.; Xu, Z.; Li, Z.; Shao, X. *ChemBioChem* **2024**, *25*, e202300742.
https://doi.org/10.1002/cbic.202300742
46. Xu, H.; Ohoka, N.; Inoue, T.; Yokoo, H.; Demizu, Y. *Bioorg. Med. Chem. Lett.* **2024**, *107*, 129788.
https://doi.org/10.1016/j.bmcl.2024.129778
47. Zhu, Y.; Yan, X.; Shi, Y.; Liu, B.; Huang, W.; Chu, L. *Bioorg. Chem.* **2024**, *143*, 107050.
https://doi.org/10.1016/j.bioorg.2023.107050
48. Jiang, G. Y.; Lei, W. H.; Zhou, Q. X.; Hou, Y. J.; Wang, X. S. *Photochem. Photobiol. Sci.* **2012**, *11*, 715.
https://doi.org/10.1039/c2pp05352g
49. Gopalakrishnan, D.; Srinath, S.; Baskar, B.; Bhuvanesh, N. S. P.; Ganeshpandian, M. *Appl. Organomet. Chem.* **2019**, *33*, e4756.
https://doi.org/10.1002/aoc.4756
50. Kitamura, T.; Shiroshita, S.; Takahashi, D.; Toshima, K. *Chem. - Eur. J.* **2020**, *26*, 14351.
https://doi.org/10.1002/chem.202000833
51. Kitamura, T.; Okuyama, M.; Takahashi, D.; Toshima, K. *Chem. - Asian J.* **2019**, *14*, 1409.
https://doi.org/10.1002/asia.201900203
52. Tsumura, K.; Suzuki, A.; Tsuzuki, T.; Tanimoto, S.; Kaneko, H.; Matsumura, S.; Imoto, M.; Umezawa, K.; Takahashi, D.; Toshima, K. *Org. Biomol. Chem.* **2011**, *9*, 6357.
https://doi.org/10.1039/c1ob05629h

53. Suzuki, A.; Tsumura, K.; Tsuzuki, T.; Matsumura, S.; Toshima, K. *Chem. Commun.* **2007**, 4260. https://doi.org/10.1039/b708947c
54. Hasegawa, M.; Suzuki, A.; Matsumura, S.; Toshima, K. *Sci. Technol. Adv. Mater.* **2006**, *7*, 169. https://doi.org/10.1016/j.stam.2005.11.024
55. Takagi, R.; Takeda, A.; Takahashi, D.; Toshima, K. *Chem. - Asian J.* **2017**, *12*, 2656. https://doi.org/10.1002/asia.201701004
56. Stromer, B.; Limbacher, M.; Jayaram, D. T.; Yenjai, S.; Chowdhury, R.; Buranaprapuk, A.; Ramaiah, D.; Kumar, C. V. *J. Photochem. Photobiol. A Chem.* **2017**, *340*, 181. https://doi.org/10.1016/j.jphotochem.2017.01.027
57. Yenjai, S.; Kuno, M.; Samosorn, S.; Liwporncharoenvong, T.; Buranaprapuk, A. *J. Photochem. Photobiol. B Biol.* **2017**, *173*, 35. https://doi.org/10.1016/j.jphotobiol.2017.05.029
58. Yenjai, S.; Kumar, C. V.; Kuno, M.; Liwporncharoenvong, T.; Samosorn, S.; Buranaprapuk, A. *J. Photochem. Photobiol. B Biol.* **2018**, *186*, 23. https://doi.org/10.1016/j.jphotobiol.2018.07.001
59. Peng, K.-C.; Chang, K.-C.; Ke, S.-C.; Chen, J.; Liu, S.-Y. *J. Photochem. Photobiol.* **2020**, *3–4*, 100008. https://doi.org/10.1016/j.jpap.2020.100008
60. Sotokawa, S.; Kitamura, T.; Takahashi, D.; Toshima, K. *Chem. Commun.* **2018**, *54*, 10614. https://doi.org/10.1039/C8CC06130K
61. Takahashi, D.; Nagao, T.; Sotokawa, S.; Toshima, K. *MedChemComm* **2016**, *7*, 1224. https://doi.org/10.1039/C6MD00167J
62. Okuyama, M.; Ueno, H.; Kobayashi, Y.; Kawagishi, H.; Takahashi, D.; Toshima, K. *Chem. Commun.* **2016**, *52*, 2169. https://doi.org/10.1039/C5CC09542E
63. Aoki, Y.; Tanimoto, S.; Takahashi, D.; Toshima, K. *Chem. Commun.* **2013**, *49*, 1169. https://doi.org/10.1039/c2cc38742e
64. Suzuki, A.; Hasegawa, M.; Ishii, M.; Matsumura, S.; Toshima, K. *Bioorg. Med. Chem. Lett.* **2005**, *15*, 4624. https://doi.org/10.1016/j.bmcl.2005.05.137
65. Wuest, F.; Bouvet, V.; Mai, B.; Lapointe, P. *Org. Biomol. Chem.* **2012**, *10*, 6724. https://doi.org/10.1039/c2ob25744k
66. Santosh Kumar, S. C.; Vijendra Kumar, N.; Srinivas, P.; Bettadaiah, B. K. *Synthesis* **2014**, *46*, 1847. https://doi.org/10.1055/s-0034-1378350
67. Nishikawa, Y.; Takemoto, K.; Matsuda, K.; Tanaka, R.; Arashima, A.; Ito, K.; Kamezawa, Y.; Hori, Y.; Hara, O. *Org. Lett.* **2018**, *20*, 3367. https://doi.org/10.1021/acs.orglett.8b01288
68. Wang, D.; Ren, S.; Wang, H.; Yan, H.; Feng, J.; Zhang, X. *Chem. Biodiversity* **2014**, *11*, 886. https://doi.org/10.1002/cbdv.201300212
69. Guo, Y.; Yang, R.; Xu, H. *RSC Adv.* **2017**, *7*, 28009. https://doi.org/10.1039/C7RA03588H
70. Sun, G. S.; Xu, X.; Jin, S. H.; Lin, L.; Zhang, J. J. *Molecules* **2017**, *22*, 958. https://doi.org/10.3390/molecules22060958
71. Zheng, Y.; Zhu, L.; Fan, L.; Zhao, W.; Wang, J.; Hao, X.; Zhu, Y.; Hu, X.; Yuan, Y.; Shao, J.; Wang, W. *Eur. J. Med. Chem.* **2017**, *125*, 902. https://doi.org/10.1016/j.ejmech.2016.10.012
72. Chalothorn, T.; Rukachaisirikul, V.; Phongpaichit, S.; Pannara, S.; Tansakul, C. *Tetrahedron Lett.* **2019**, *60*, 151004. https://doi.org/10.1016/j.tetlet.2019.151004
73. Nicolaou, K. C.; Baran, P. S.; Zhong, Y. L. *J. Am. Chem. Soc.* **2001**, *123*, 3183.

https://doi.org/10.1021/ja004218x
74. Trump, E. L.; Xiaohong Zhou, M. *Trans. Kansas Acad. Sci.* **1993**, *96*, 167. https://doi.org/10.2307/3628136
75. Maity, A. C. *Synlett* **2008**, 465. https://doi.org/10.1055/s-2008-1032130
76. Illescas, B. M.; Martín, N. *J. Org. Chem.* **2000**, *65*, 5986. https://doi.org/10.1021/jo0003753
77. Wolfe, A.; Shimer, G. H. J.; Meehan, T. *Biochemistry* **1987**, *26*, 6392. https://doi.org/10.1021/bi00394a013
78. Luis García-Giménez, J.; González-Álvarez, M.; Liu-González, M.; Macías, B.; Borrás, J.; Alzuet, G. *J. Inorg. Biochem.* **2009**, *103*, 923. https://doi.org/10.1016/j.jinorgbio.2009.04.003
79. Phadte, A. A.; Banerjee, S.; Mate, N. A.; Banerjee, A. *Biochem. Biophys. Rep.* **2019**, *18*, 100629. https://doi.org/10.1016/j.bbrep.2019.100629
80. Barkhudaryan, V. G.; Ananyan, G. V. *J. Biomol. Struct. Dyn.* **2020**, *38*, 3489. https://doi.org/10.1080/07391102.2019.1660217
81. Dimitrakopoulou, A.; Dendrinou-Samara, C.; Pantazaki, A. A.; Alexiou, M.; Nordlander, E.; Kessissoglou, D. P. *J. Inorg. Biochem.* **2008**, *102*, 618. https://doi.org/10.1016/j.jinorgbio.2007.10.005
82. Lakowicz, J. R. *Principles of fluorescence spectroscopy, 3rd Principles of fluorescence spectroscopy, Springer, New York, USA, 3rd edn, 2006.*; **2006**. https://doi.org/10.1007/978-0-387-46312-4
83. Heller, D. P.; Greenstock, C. L. *Biophys. Chem.* **1994**, *50*, 305. https://doi.org/10.1016/0301-4622(93)E0101-A
84. Jones, M. N.; Skinner, H. A.; Tipping, E. *Biochem. J.* **1975**, *147*, 229. https://doi.org/10.1042/bj1470229
85. Rabbani, G.; Ahn, S. N. *Int. J. Biol. Macromol.* **2019**, *123*, 979. https://doi.org/10.1016/j.ijbiomac.2018.11.053
86. Xu, Z.; Liu, Y.; Zhou, S.; Fu, Y.; Li, C. *Int. J. Mol. Sci.* **2016**, *17*, 1042. https://doi.org/10.3390/ijms17071042
87. Zhang, J.; Gao, X.; Huang, J.; Wang, H. *ACS Omega* **2020**, *5*, 16833. https://doi.org/10.1021/acsomega.0c02031
88. Barakat, K.; Ragheb, M. A.; Soliman, M. H.; Abdelmoniem, A. M.; Abdelhamid, I. A. *BMC Chem.* **2024**, *18*. https://doi.org/10.1186/s13065-024-01284-2
89. Siddiqui, S.; Ameen, F.; ur Rehman, S.; Sarwar, T.; Tabish, M. *J. Mol. Liq.* **2021**, *336*, 116200. https://doi.org/10.1016/j.molliq.2021.116200
90. Stella, L.; Capodilupo, A. L.; Bietti, M. *Chem. Commun.* **2008**, 4744. https://doi.org/10.1039/b808357f
91. Shamsi, A.; Mohammad, T.; Anwar, S.; Alajmi, M. F.; Hussain, A.; Hassan, M. I.; Ahmad, F.; Islam, A. *Int. J. Biol. Macromol.* **2020**, *148*, 533. https://doi.org/10.1016/j.ijbiomac.2020.01.134
92. Laitinen, O. H.; Hytönen, V. P.; Nordlund, H. R.; Kulomaa, M. S. *Cell. Mol. Life Sci.* **2006**, *63*, 2992. https://doi.org/10.1007/s00018-006-6288-z
93. Lukeman, M.; Xu, M.; Wan, P. *Chem. Commun.* **2002**, 136. https://doi.org/10.1039/b108746k
94. Elian, C.; Sanosa, N.; Bogliotti, N.; Herrero, C.; Sampedro, D.; Versace, D.-L. *Polym. Chem.* **2023**, *14*, 3262. https://doi.org/10.1039/D3PY00681F

